Exploring mechanisms that affect coral cooperation: symbiont transmission mode, cell density and community composition

Carly D Kenkel[a,1] and Line K Bay[b,2]

[a]Department of Biological Sciences, University of Southern California, 3616 Trousdale Parkway, Los Angeles, CA 90089, USA

[b]Australian Institute of Marine Science, PMB No 3, Townsville MC, Queensland 4810, Australia

[1]Corresponding author, email: ckenkel@usc.edu; phone: 213-821-1705; fax: 213-740-8123

[2]Email: L.Bay@aims.gov.au

RUNNING TITLE: coral-algal cooperation mechanisms

KEYWORDS: Symbiosis, transmission mode, reef corals, bleaching, carbon translocation

DATA ARCHIVAL LOCATION: Raw amplicon sequencing data have been uploaded to NCBI's SRA: PRJNA338365. All R scripts and input files have been included as supplementary files for review and will be uploaded to Zenodo upon publication DOI: 10.5281/zenodo.1208684.

ABSTRACT

The coral symbiosis is the linchpin of the reef ecosystem, yet the mechanisms that promote and maintain cooperation between hosts and symbionts have not been fully resolved. We used a phylogenetically controlled design to investigate the role of vertical symbiont transmission, an evolutionary mechanism in which symbionts are inherited directly from parents, predicted to enhance cooperation and holobiont fitness. Six species of coral, three vertical transmitters and their closest horizontally transmitting relatives, which exhibit environmental acquisition of symbionts, were fragmented and subjected to a two-week thermal stress experiment. Symbiont cell density, photosynthetic function and translocation of photosynthetically fixed carbon between symbionts and hosts were quantified to assess changes in physiological performance and cooperation. All species exhibited similar decreases in symbiont cell density and net photosynthesis in response to elevated temperature, consistent with the onset of bleaching. Yet baseline cooperation, i.e. translocation of photosynthate, in ambient conditions and the reduction in cooperation in response to elevated temperature differed among species. Although *Porites lobata* and *Galaxea acrhelia* did exhibit the highest levels of baseline cooperation, we did not observe universally higher levels of cooperation in vertically transmitting species. *Post hoc* sequencing of the *Symbiodinium* ITS-2 locus was used to investigate the potential role of differences in symbiont community composition. Interestingly, reductions in cooperation at the onset of bleaching tended to be associated with increased symbiont community diversity among coral species. The theoretical benefits of evolving vertical transmission are based on the underlying assumption that the host-symbiont relationship becomes genetically uniform, thereby reducing competition among symbionts. Taken together, our results suggest that it may not be vertical transmission *per se* that influences host-symbiont cooperation, but genetic uniformity of the symbiont community, although additional work is needed to test this hypothesis.

INTRODUCTION

Cooperation between species has played a fundamental role in the evolution and diversification of life (Friesen & Jones 2013; Kiers & West 2015; Maynard Smith & Szathmary 1995; Moran 2006). In the case of reef-building corals, the intracellular symbiosis between dinoflagellates in the genus *Symbiodinium* and a calcifying Cnidarian host forms the basis of one of the most biodiverse and productive ecosystems on the planet (Hatcher 1988; Knowlton et al. 2010). The process of host calcification, which builds the three dimensional structure of the reef, is largely powered by symbiont primary productivity (Roth 2014). However, climate change and other anthropogenic processes threaten reefs because of the sensitivity of the coral-dinoflagellate symbiosis to environmental stress (Hoegh-Guldberg et al. 2007; Hughes et al. 2003), indicating that host-symbiont cooperation is not stable over ecological timescales.

Recent work has suggested that a transition to parasitism may precipitate the breakdown of the host-symbiont relationship (Baker et al. 2018), but this is not a unique feature of the coral symbiosis. Across taxa, mutualisms are better defined as a spectrum that ranges from negative parasitic interactions to mutually beneficial symbioses, both within the context of a focal inter-species interaction and when comparing relationships across taxa (Doebeli & Knowlton 1998; Lesser et al. 2013; Nowak et al. 1994; Sachs et al. 2011). Less well-resolved, particularly for the coral-*Symbiodinium* symbiosis, are the mechanisms that promote and maintain positive interactions between partners (Lesser et al. 2013; Sachs & Wilcox 2006).

One major factor predicted to influence levels of cooperation is the mode of symbiont transmission (Anderson & May 1982; Ebert & Bull 2003). In corals as in other symbioses, two transmission modes predominate: symbionts can be acquired horizontally from the local

environment, usually during a defined larval stage, or vertically from parents, typically through the maternal germ line (reviewed in (Bright & Bulgheresi 2010). Virulence theory predicts that horizontal transmission allows symbionts to adopt selfish strategies, potentially harmful to the host (Bull 1994). A transition from horizontal to vertical transmission is predicted to align the reproductive interests of partners (via partner-fidelity feedback *sensu* (Sachs et al. 2004) and optimize resource sharing to maximize holobiont (the combination of host and symbiont) fitness (Ebert 2013; Frank 1994; Herre et al. 1999).

Experimental manipulations of transmission mode in other systems have provided empirical support for a reduction in pathogen virulence under enforced vertical transmission scenarios (Bull et al. 1991; Dusi et al. 2015; Sachs & Wilcox 2006; Stewart et al. 2005). Bacteriophages forced into vertical transmission evolved lower virulence and lost the capacity to transmit horizontally (Bull et al. 1991). Similarly, *Symbiodinium microadriaticum* under an experimentally enforced horizontal transmission regime proliferated faster within their *Cassiopea* jellyfish hosts while reducing host reproduction and growth (Sachs & Wilcox 2006). However, studies attempting to quantify the evolutionary consequences of natural shifts in transmission mode remain rare, with Herre's demonstration of a negative relationship between vertical transmission and virulence in nematodes that parasitize fig wasps a notable exception (Herre 1993).

Reef-building corals are a potential system in which to study naturally occurring transitions in transmission mode in a mutualistic symbiosis. Corals (Cnidaria: Anthozoa: Scleractinia) are colonial animals that harbour intracellular populations of dinoflagellate algae in the genus *Symbiodinium*. This symbiosis is considered obligate as the breakdown of the relationship between host animals and their intracellular *Symbiodinium* algae, commonly known as coral bleaching, has major fitness consequences for both partners, and can be lethal (reviewed in (Brown 1997). This inter-species partnership is ancient (evolved ~ 250 MYA

75 (Stanley & Swart 1995), prolific (600+ coral species worldwide (Daly et al. 2007), and
76 constitutes the foundation of one of the most bio-diverse ecosystems on the planet. The
77 majority of coral species (~85%) acquire their *Symbiodinium* horizontally from the local
78 environment in each generation (Harrison & Wallace 1990). However, vertical transmission
79 has independently evolved at least four times, such that both transmission strategies can be
80 exhibited by different coral species within the same genus (Baird et al. 2009b; Hartmann et
81 al. 2017).

82 We compared physiological components of cooperation and fitness proxies between
83 horizontal and vertical transmitters in a phylogenetically controlled design using three pairs
84 of related coral species exhibiting different strategies: (1) *Galaxea acrhelia* (vertical
85 transmitter, VT) and *G. astreata* (horizontal transmitter, HT); (2) *Porites lobata* (VT) *and*
86 *Goniopora columna* (HT); (3) *Montipora aequituberculata* (VT) *and Acropora millepora*
87 (HT). Species comparisons were drawn from the same or sister genera and replicate
88 comparisons from more distantly related clades (Hartmann et al. 2017). Species also
89 represented a diversity of reproductive modes (e.g. broadcast spawner, brooder), sexual
90 systems (e.g. hermaphroditic, gonochoric), and morphologies (e.g. massive, branching), and
91 host different subclades of *Symbiodinium* (Tonk et al. 2013), such that mode of symbiont
92 transmission was the only consistent difference between pairs (Baird et al. 2009b; Franklin et
93 al. 2012; Kerr et al. 2011). We quantified changes in symbiont cell density, photosynthetic
94 function and translocation of photosynthetically fixed carbon between symbionts and hosts.
95 We defined cooperation as the proportion of photosynthetically fixed carbon translocated to
96 the host, while the degree of symbiont parasitism was calculated as the difference in the
97 proportion of photosynthetically fixed carbon translocated to hosts between control and heat-
98 treated samples at the end of the experiment, *sensu* Baker et al. (2018). Bleaching, or the
99 reduction in symbiont density in response to sustained thermal stress was used as a proxy for

100 holobiont fitness. While we observed differences in host-symbiont cooperation, both at a
101 baseline level and during the onset of bleaching, vertically transmitting species did not
102 exhibit universally elevated levels of cooperation. Additional *post hoc* analysis of
103 *Symbiodinium* ITS-2 diversity among coral species was therefore used to investigate whether
104 symbiont community composition could better explain physiological trait patterns. Symbiont
105 community composition did not explain a significant portion of the variation in physiological
106 components of cooperation or fitness proxies; however, diversity tended to be associated with
107 the degree of symbiont parasitism at the onset of bleaching, suggesting that reduced genetic
108 diversity of symbionts, rather than vertical transmission *per se*, may influence host-symbiont
109 cooperation.

110 MATERIALS and METHODS

111 *Coral Collection and Acclimation*

112 Fragments from sixty unique coral colonies, ~ 20 cm in diameter, were collected from
113 reefs on the Central GBR from the 8-22 April 2015 under the Great Barrier Reef Marine Park
114 Authority permits G12/35236.1 and G14/37318.1, prioritizing collection of focal species
115 pairs by transmission mode from the same reef environment, including location and depth.
116 Ten corals of each species, *Galaxea acrhelia* and *G. astreata* were collected from Davies
117 Reef (18°49.816', 147°37.888', 11 April 2015), ten corals each of *Acropora millepora* and
118 *Montipora aequituberculata* were collected from Pelorus Island (18°33.358', 146°30.276', 18
119 April 2015) and ten corals each of *Goniopora columna* and *Porites lobata* were collected
120 from Pandora Reef (18°48.778', 146°25.593', 21 April 2015) from depths of <10m across all
121 reefs, and from the same depth within each site. Corals were transported to the Australian
122 Institute of Marine Science Sea Simulator facility and placed in shaded outdoor holding tanks
123 with 0.2 µM filtered flow-through seawater (FSW, 27°C, 150 µmol quanta m^{-2} s^{-1}). Each

124 individual coral colony was further cut into 6 replicates using a diamond blade band saw and
125 these fragments were mounted on aragonite plugs using either super-glue or marine epoxy.
126 On 1 May 2015, fragments were moved into indoor experimental aquaria, which consisted of
127 12 50-L treatment tanks fitted with 3.5-watt Turbelle nanostream 6015 pumps (Tunze,
128 Germany) with flow-through filtered seawater (FSW, ~25 liters/hour) at 27°C with Hydra 52
129 lights (Aqua Illumination, C2 Development, Inc., USA) on a 12:12 light/dark cycle
130 mimicking natural irradiance patterns, peaking at 130-160 µmol quanta m^{-2} s^{-1} at "midday",
131 which actually occurred at 10:30 GMT+10. Tanks, coral racks and plugs were cleaned daily.
132 Beginning on 7 May, at 20 mins before dark (16:30 GMT +10) every day, corals were fed
133 *Artemia* naupli at a density of 1-1.5 naupli/5ml and rotifers at a density of 1-3/ml.

134 *Experimental Conditions and Physiological Trait Measurements*

135 Beginning on 28 May 2015, effective quantum yield of *Symbiodinium* photosystem II
136 (EQY) was measured daily for all experimental fragments using a pulse amplitude modulated
137 fluorometer (diving-PAM, Walz) fitted with a plastic fibre optic cable (Fig. S1).
138 Measurements were made using factory settings with a measuring intensity of 12 and a gain
139 of 5 and taken at peak light intensity (between 09:30 – 1130 GMT +10). EQY values were
140 used to guide the timing of the final sampling time point (Fig. S2), where a decline reflects an
141 impact on the photosynthetic condition of the *Symbiodinium* (Ralph et al. 2005) because we
142 aimed to target the onset of the coral bleaching response rather than the end-point.

143 On 31 May 2015, temperatures in the heat treatment tanks were increased at a rate of
144 1°C per day until temperatures reached 31°C (day 4, Fig S3). Sample time points occurred on
145 day 2 (29°C, 1 Jun), day 4 (31°C, 3 Jun) and day 17 (31°C, 16 Jun, Fig S3). On each
146 sampling day, one replicate fragment of each colony (n=10) and species (n=6) from each
147 temperature treatment (n=2; n=120 total per sampling day) were used to measure net

148 photosynthesis following the two-point method originally described and validated for *A.*
149 *millepora* in Strahl et al. (2015). It is important to note that this method was not validated for
150 additional species or under the experimental conditions used in the present study, nor were
151 species specific photosynthesis-irradiance curves quantified to determine an appropriate
152 saturating irradiance. Briefly, corals were incubated in enclosed 600-ml acrylic chambers at
153 their respective treatment temperatures and light levels for 1.5 h. Chambers were placed onto
154 custom built tables with rotating magnets, which served to power stir bars within each
155 chamber to facilitate water mixing. For each run, four chambers without corals were used as
156 blanks to account for potential changes in oxygen content due to the metabolic activity of
157 other microorganisms in the seawater. For net photosynthesis measures, the O_2 concentration
158 of the seawater in each chamber was measured at the end of the run using a hand-held
159 dissolved oxygen meter (HQ30d, equipped with LDO101 IntelliCAL oxygen probe, Hach,
160 USA). Values from blank chambers were subtracted from measures made in coral chambers
161 and the subsequent rate of net photosynthesis was related to coral surface area, calculated in
162 μg $O_2/cm^2/min$.

163 To measure the fraction of autotrophically derived carbon translocated to host
164 animals, five colony fragments of each species from each treatment (n=30 control, n=30 heat)
165 were placed into 18-L of FSW with a 5-W aquarium pump for circulation and ^{14}C-
166 bicarbonate (specific activity: 56 mCi/mmol) was added to a final concentration of 0.28
167 μCi/ml. Corals were incubated for 5 hours in experimental tanks which experienced the
168 normal experimental irradiance profile from 09:00 – 1400 GMT +10, rinsed with flow-
169 through FSW for one hour to remove remaining unfixed ^{14}C then snap frozen in liquid
170 nitrogen.

171 Tissue was removed from snap frozen coral skeletons using an air gun and
172 homogenized for 60 s using a Pro250 homogenizer (Perth Scientific Equipment, AUS). A

173 300-µl aliquot of the tissue homogenate was fixed with 5% formalin in FSW and used to
174 quantify *Symbiodinium* cell density. The average cell number was obtained from four
175 replicate haemocytometer counts of a 1-mm^3 area and cell density was related to host protein
176 content (as assessed below) and expressed as cells/mg host protein. Although surface area is
177 common used as the normalization factor for *Symbiodinium* cell density, it has been
178 recognized that areal abundance does not account for differences in host biomass (reviewed
179 in (Cunning & Baker 2014). We found that normalization to soluble host protein more
180 accurately reflected this difference in biomass, given that tissue thickness is significantly
181 greater in *Goniopora columna* and not adequately accounted for by skeletal surface area
182 normalization alone (Fig. S4). We determined the degree of bleaching, or the reduction in
183 symbiont density in response to sustained thermal stress, by calculating the difference in
184 symbiont cell densities between heat-treated and paired control samples following the full 17
185 days of experimental treatment and used this value as a proxy of holobiont fitness.

186 An additional 1-ml aliquot of holobiont homogenate was frozen at -20°C. The
187 remaining homogenate was centrifuged for 2 min at 3500 rcf to separate host and symbiont
188 fractions and 2-ml of the host tissue slurry was frozen at -20°C. Total soluble protein was
189 quantified for host tissue samples in duplicate using a colorimetric assay (Bio-Rad Protein
190 Assay Kit II, USA) following the manufacturer's instructions. Coral skeletons were rinsed
191 with 5% bleach then dried at room temperature. Skeletal surface area was quantified using
192 the single wax dipping method (Veal et al. 2010) and skeletal volume (used to standardize
193 respirometry chamber volumes) was determined by calculating water displacement in a
194 graduated cylinder.

195 Sample radioactivity was determined using a liquid scintillation counter (Tri-Carb
196 2810TR v2.12, Perkin Elmer, USA). Triplicate host and duplicate holobiont 300 µl tissue
197 homogenate aliquots were mixed with 3.5 ml Ultima Gold XR liquid scintillation cocktail

198 (Perkin Elmer, USA). Samples were temperature and light adapted for 1 hour and then
199 counted for 1.5 min using the default parameters. Counts per minute were converted to
200 disintegrations per minute (DPM) using a standard curve derived from a ^{14}C Ultima Gold
201 Quench Standards Assay (Perkin Elmer, USA). Technical replicates were averaged. Host
202 DPM values were divided by holobiont DPM values to yield the fraction of autotrophically
203 derived carbon shared between partners, which we defined as our metric of host-symbiont
204 cooperation. The degree of symbiont parasitism was calculated as the difference in this
205 proportion of photosynthetically fixed carbon translocated to hosts between heat-treated and
206 paired control samples following the full 17 days of experimental treatment, *sensu* Baker et
207 al. (2018).

208 To identify major *Symbiodinium* clades hosted by focal species, DNA was extracted
209 from symbiont fractions of the tissue homogenate for each replicate colony of each species
210 (n=60, all control tank fragments) using Wayne's method (Wilson et al. 2002). A restriction
211 digest of the LSU region of *Symbiodinium* rRNA (Baker & Rowan 1997; Palstra 2000)
212 consistently revealed single bands indicating the dominance of a single *Symbiodinium* clade
213 for four of the six species (*A. millepora*, *M. aequituberculata*, *G. columna* and *P. lobata*)
214 whereas communities in *G. astreata* and *G. acrhelia* appeared more variable (Fig. S5).
215 Therefore, DNA was pooled in equal proportions by species (n=6 samples) to identify
216 general species-specific communities using amplicon sequencing of the ITS2 region of
217 *Symbiodinium* rRNA. Additional DNA samples for each of the *G. astreata* and *G. acrhelia*
218 colony replicates (n=20 samples) were also submitted for sequencing at the Genome
219 Sequencing and Analysis Facility at the University of Texas at Austin. Given the high
220 diversity subsequently observed in pooled samples of *P. lobat*a and *M. aequituberculata*,
221 additional colony replicate samples of each (n=3 and n=5, respectively) were later submitted

222 for sequencing at Oregon State University's Center for Genome Research and Biocomputing
223 to compare symbiont community composition from individual samples.

224 *Amplicon Sequencing Analysis*

225 For sample libraries prepared and sequenced at UT Austin's GSAF, the ITS2 primers
226 of Pochon et al. (Pochon et al. 2001) were used. For colony replicate samples sequenced at
227 OSU's CGRB (individual *P. lobata* and *M. aequituberculata* samples), the ITS2 primers of
228 LaJeunesse (LaJeunesse 2002) were used to prepare libraries. All sequencing libraries were
229 subsequently analyzed together. Prior to analysis, raw read data was filtered to remove reads
230 which contained Illumina sequencing adapters or did not begin with the correct ITS2
231 amplicon primer sequence using the BBMAP package ver. 37.75
232 (http://sourceforge.net/projects/bbmap/). The DADA2 pipeline (Callahan 2016) implemented
233 in R (Team 2017) was then used to infer sequence variants. Read data was analyzed
234 according to the following tutorial (https://benjjneb.github.io/dada2/tutorial.html) with the
235 following modifications: ITS2 primers were trimmed from the beginning of each read and
236 forward and reverse reads were truncated at 210bp and 160bp respectively to remove low
237 quality bases at the end of reads. Additional paired end reads were discarded if they exhibited
238 more than one expected error or when a quality score of 2 or less was encountered. In
239 addition, when inferring sequencing variants using the *dada*() command, the BAND_SIZE
240 flag was set to 32 as is recommended for ITS data
241 (https://benjjneb.github.io/dada2/tutorial.html). The distribution of raw read data per sample
242 and reads lost during quality filtering and processing steps can be found in Table S1. Post-
243 clustering curation of identified amplicon sequence variants (ASVs) was accomplished with
244 the LULU algorithm, using the default parameters (Frøslev et al. 2017). The MCMC.OTU
245 package (Green et al. 2014) was then used to remove sample outliers with low counts overall
246 (z-score <-2.5) and remaining ASVs of abundance less than 0.001 (Quigley et al. 2014) prior

247 to statistical analysis. In total, 12 ASVs were identified across samples that satisfied these
248 criteria. These high confidence sequence variants were taxonomically classified through a
249 blast search against the GeoSymbio ITS2 database
250 https://sites.google.com/site/geosymbio/downloads (Franklin et al. 2012), and the best match
251 was recorded. In cases where variants matched equally well to multiple references, all top hits
252 were reported (Table S2). Resequencing of the individual *P. lobata* and *M. aequituberculata*
253 samples indicated that the *P. lobata* pooled sample was contaminated at some stage of the
254 sequencing process, as individual samples did not match the host pool (Fig. S6). In addition,
255 two *Galaxea* samples (Gacr1 and Gast4) appeared mislabeled, based on the pattern of
256 symbiont community differences among species (Fig S6) and we removed these samples
257 prior to further analysis. To account for differences between individual samples and species
258 pools, we calculated the normalized mean abundance of each variant across individual
259 samples within a species and replaced the pooled sequence sample with this *in silico* pooled
260 value, when available.

261 *Statistical Analyses*

262 All statistical analyses were performed in R, version 3.4.2 (Team 2017). A series of
263 linear mixed models were used to determine the effect of species, temperature treatment and
264 sampling day on physiological metrics. We used a conservative approach to evaluate the
265 effect of transmission mode on physiological metrics. Rather than modelling fixed effects of
266 transmission mode directly, we modelled the fixed effects of species (levels: Amil, Maeq,
267 Gcol, Plob, Gast, Gacr), sampling day (levels: day 2, day 4, day 17), temperature treatment
268 (levels: heat, control) and all possible interactions on *Symbiodinium* cell density, net
269 photosynthesis, and host-symbiont resource sharing using the *lme* command of the *nlme*
270 package (Pinheiro et al. 2013), including source coral colony identity nested within reef of
271 origin as a scalar random factor. All models were assessed for normality of residuals and

homoscedasticity. Symbiont densities required a log-transformation to meet normality assumptions. To assess goodness-of-fit, we used the function *rsquared.glmm* to calculate the conditional R^2 value for each of our mixed models (Johnson 2014). Significance of fixed factors within models was evaluated using Wald tests and Tukey's post-hoc tests were used to evaluate significance among levels within factors and interactions when warranted. In these models, a significant effect of transmission mode would have been detected first as a significant difference among species, but significant differences in the hypothesized direction between each pair of vertical and horizontal transmitters in the subsequent Tukey's tests were also required to satisfy reporting an effect of transmission mode overall.

To determine the impact of specific *Symbiodinium* community characteristics on responses among species, the DESeq package (Anders & Huber 2010) was used to construct a series of generalized linear models to evaluate differences in in the abundance of each ASV by species with respect to aspects of host-symbiont cooperation: mean initial symbiont density (Day 2, heat samples); the mean fraction of carbon shared by symbionts under ambient conditions (Day 2, 4, 17 control samples), the mean difference in the fraction of carbon shared by symbionts during bleaching (Day17, heat vs. control samples) and the mean difference in symbiont density during bleaching (Day17, heat vs. control samples). Models were run for 30 iterations and for models that did not converge, p-values were converted to NAs, the standard notation for missing data, prior to applying a multiple test correction (Benjamini & Hochberg 1995).

Predictive relationships between *Symbiodinium* cell density, the degree of bleaching, cooperation, and symbiont parasitism, in addition to *Symbiodinium* community diversity (quantified using the inverse Simpson index, (Magurran 2004)) and composition (the proportion of Clade D) were explored at the species level using a series of linear models. When a significant difference was detected among species for physiological trait

297 comparisons, the model was re-run within each species and a multiple test correction using
298 the method of Benjamini & Hochberg (1995) was applied. Analyses of symbiont community
299 composition were run both using the full six species averages and excluding the species for
300 which individual sample sequencing replicates were not available (*A. millepora* and *G.*
301 *columna*). As models did not substantially differ, we report results for the full six species.

302 RESULTS

303 *Physiological metrics of thermal tolerance and cooperation*

304 Significant fixed effects of species, temperature treatment, sampling time and the
305 time*treatment interaction were detected for the *Symbiodinium* cell density model
306 (R^2_{GLMM}=0.53, Table S3). The fixed difference among species was driven by the low
307 symbiont density on average in *P. lobata*, which differed significantly from densities in *A.*
308 *millepora*, *M. aequituberculata*, *G. astreata* and *G. acrhelia* (Tukey's HSD < 0.05, Fig. 1).
309 No differences were detected in post-hoc tests between focal species pairs by symbiont
310 transmission mode. Across species, cell densities did not differ between control and heat-
311 treated corals on days 2 and 4, but were reduced in heat treated corals on day 17, by 5.4 x 10^5
312 cells/mg host protein on average (Tukey's HSD < 0.001, Fig. 1).

313 The model for changes in the rate of net photosynthesis identified significant effects
314 of species, sampling time and the temperature treatment*time interaction (R^2_{GLMM}=0.53,
315 Table S4). Average net O_2 production rate was highest in *M. aequituberculata,* differing
316 significantly from *A. millepora, G. columna*, *G. acrhelia,* and *P. lobata* Tukey's HSD < 0.05,
317 Fig. 1), and lowest in *G. columna*, significantly more so in comparison to *M.*
318 *aequituberculata, P. lobata, G. astreata and G. acrhelia* (Tukey's HSD < 0.001, Fig. 1). Net
319 O_2 production rate was also lower on average in *A. millepora* than in *M. aequituberculata* and
320 *G. astreata* (Tukey's HSD < 0.01, Fig. 1). Considering differences between focal species

321 pairs by symbiont transmission mode, the rate of net photosynthesis was significantly higher
322 in the vertically transmitting *M. aequituberculata* and *P. lobata* than in their horizontally
323 transmitting counterparts, *A. millepora* and *G. columna*. However, it is important to note that
324 absolute rates of oxygen production among focal species are much lower than previously
325 reported values for corals (e.g. (Anthony et al. 2008). Corals were acclimated to a common
326 light environment, but data on species-specific photosynthesis-irradiance curves are lacking.
327 Consequently, the differences among species may be influenced by variation in species-
328 specific photobiology.

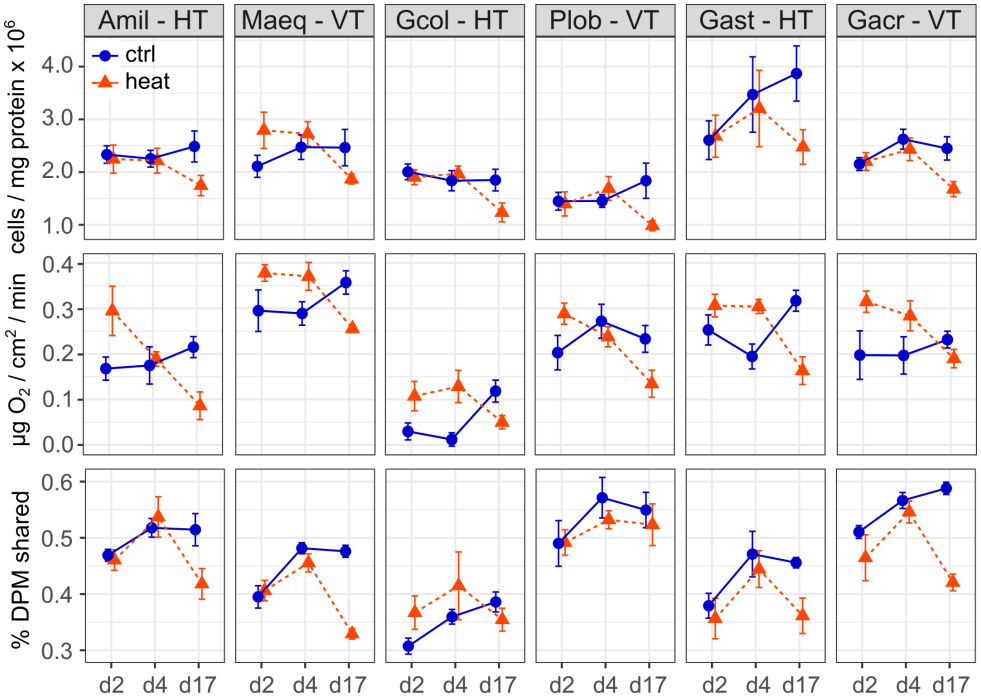

329

330 Figure 1. *Symbiodinium* cell density, expressed as cells per mg of host protein, rate of net
331 photosynthesis, expressed as mg 0_2 / cm^2 / min and the proportion of photosynthetically
332 fixed carbon translocated to the host, calculated as the ratio of total radioactivity in DPM in
333 host to holobiont tissue fractions of focal coral species (Amil: *Acropora millepora*, Maqe:
334 *Montipora aequituberculata*, Gcol: *Goniopora columna*, Plob: *Porites lobata*, Gast:
335 *Galaxea astreata*, Gach: *Galaxea acrhelia*) under control (27°C, blue circles) and elevated
336 (31°C, red triangles) temperature following 2, 4 and 17 days of treatment.

337

338 Over the course of the experiment, net photosynthesis rates were elevated in heat-
339 treated corals on days 2 and 4 relative to their respective controls (day2: 0.09 µg $O_2/cm^2/min$;

340 day 4: 0.06 µg $O_2/cm^2/min$; Tukey's HSD < 0.01, Fig. 1) and reduced in heat-treated corals
341 on day 17, by 0.1 µg $O_2/cm^2/min$ (Tukey's HSD < 0.001, Fig. 1).

342 The proportion of carbon photosynthetically fixed by symbionts then translocated to
343 hosts was significantly different among species, temperature treatment, sampling time, the
344 treatment*time interaction and the species*treatment interaction (R^2_{GLMM}=0.73, Table S5).
345 Carbon sharing in ambient conditions was significantly lower in *G. columna* in comparison to
346 all other species (Tukey's HSD < 0.05, Fig. 1) and highest in the vertically transmitting *G.*
347 *acrhelia* and *P. lobata*, significantly more so than in *M. aequituberculata* and their
348 horizontally transmitting counterparts, *G. astreata* and *G. columna* (Tukey's HSD < 0.01,
349 Fig. 1). Over time, no significant differences were detected in carbon sharing between control
350 and heat-treated corals on days 2 and 4, but proportional translocation was significantly lower
351 in heat-treated corals on day 17 (Tukey's HSD < 0.001, Fig. 1). Relative to controls, carbon
352 sharing decreased slightly under heat treatment on average in all species save *G. columna*,
353 though the only significant difference was observed in *G. acrhelia* (heat vs. control Tukey's
354 HSD < 0.01, Fig. 1). Although the species*treatment*time interaction was not significant in
355 the final model, this was likely driven by the decrease in heat-treated corals on day 17, which
356 is most evident in *A. millepora*, *M. aequituberculata, G. astreata* and *G. acrhelia*.

357 *Relationships between symbiont density, degree of bleaching and carbon translocation*

358 Symbiont cell density did not explain a significant proportion of the variance in
359 carbon translocation under ambient conditions (control corals on days 2, 4 and 17) due to
360 differences among species ($F_{1,5}$ = 25.57, P < 0.001, Fig. 2). Within species, carbon
361 translocation increased with increasing symbiont density in *G. acrhelia* (R^2=0.22) but this
362 relationship became non-significant after applying a multiple test correction.

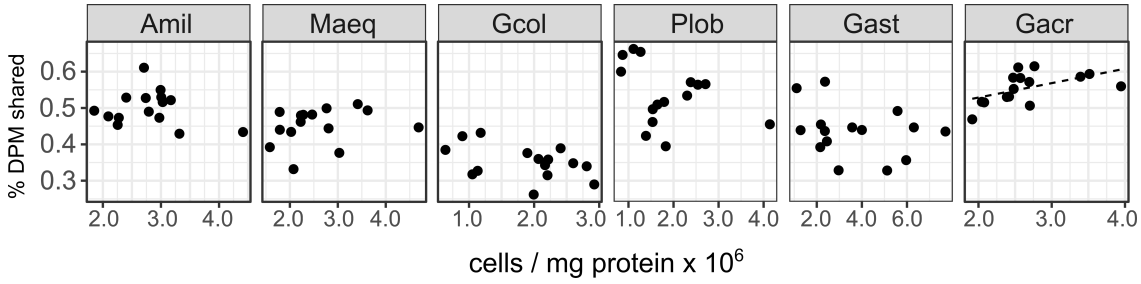

Figure 2. The proportion of photosynthetically fixed carbon translocated to the host in ambient conditions (27°C) as a function of *Symbiodinium* cell density by species (Amil: *Acropora millepora*, Maqe: *Montipora aequituberculata*, Gcol: *Goniopora columna*, Plob: *Porites lobata*, Gast: *Galaxea astreata*, Gach: *Galaxea acrhelia*).

Symbiont cell density in heat-treated corals on day 2 predicted a small portion of the variance in bleaching intensity on day 17 (calculated as the difference in cell density between paired control and heat-treated coral fragments). Greater bleaching was associated with higher initial symbiont cell densities ($\beta = -0.34$, $R^2 = 0.06$, $P = 0.04$, Fig. 3A) and this relationship did not differ significantly among species. A similar, but non-significant trend was also observed between bleaching on day 17 and symbiont cell density on day 4 ($\beta = -0.24$, $R^2 = 0.04$, $P = 0.07$).

No significant relationship was detected between the degree of bleaching and the degree of parasitism (calculated as the difference in carbon translocation between heat and control treated samples of paired corals by source colony) at the end of the experiment (Fig. 3B). Nor was the degree of parasitism explained by differences in symbiont cell density of heat-treated corals on day 2, but relationships differed among species ($F_{1,5} = 6.88$, $P < 0.001$). In *P. lobata*, a higher symbiont density on day 2 was associated with lower parasitism, or an increase in proportional carbon translocation in heat-treated corals on day 17, and this relationship remained marginally significant even after applying a multiple test correction ($R^2 = 0.89$, $P = 0.06$, Fig 3C).

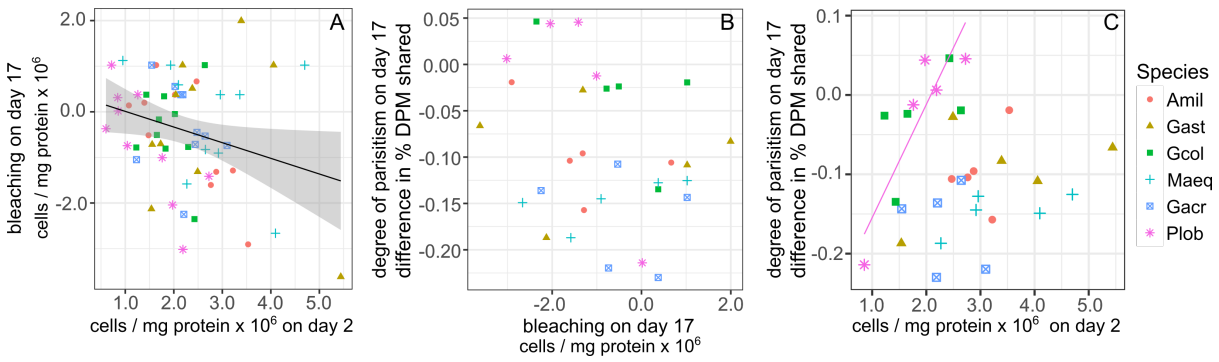

Figure 3. Relationships between changes in symbiont cell density and the proportion of photosynthetically fixed carbon translocated to hosts. (A) Bleaching intensity, calculated as the change in symbiont cell density between control (27°C) and heat-treated (31°C) samples on day 17 as a function of symbiont cell density in heat-treated corals on day 2. (B) The degree of symbiont parasitism, calculated as the difference in the proportion of photosynthetically fixed carbon translocated to hosts between control and heat-treated samples on day 17. (C) The degree of symbiont parasitism as a function of symbiont cell density in heat-treated corals on day 2. Regression line shown for Plob only. Amil: *Acropora millepora*, Maqe: *Montipora aequituberculata*, Gcol: *Goniopora columna*, Plob: *Porites lobata*, Gast: *Galaxea astreata*, Gach: *Galaxea acrhelia*.

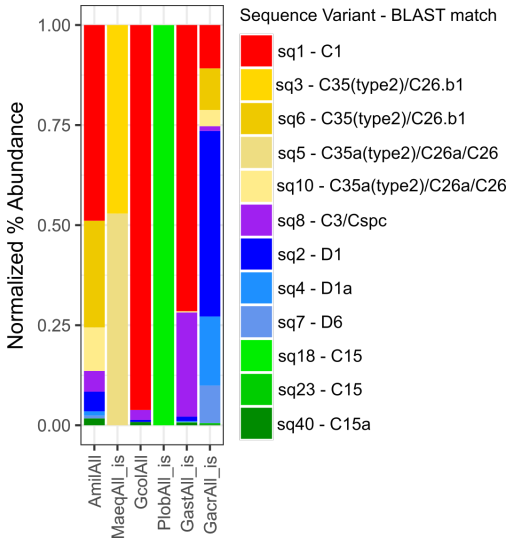

Figure 4. Normalized percent abundance of sequence variants by pooled sample. The 'is' label indicates samples for which sequence variant abundances across individually sequenced samples were pooled *in silico*. The best BLAST match against the GeoSymbio ITS2 database (Franklin et al. 2012) for each sequence variant is also reported.

The role of Symbiodinium *community composition*

Across all individual and pooled samples, 12 ASVs of sufficient representation (>0.1% abundance, *sensu* (Quigley et al. 2014) were identified and consisted of clade C and D-type *Symbiodinium* (Table S2, Fig. S6). *Symbiodinium* community composition varied

among species (Fig. 4) but no relationships were detected between the abundance of individual ASVs and symbiont density, degree of bleaching or carbon translocation. Nor did we detect any relationship between *Symbiodinium* community diversity overall and symbiont density on day 2, mean carbon translocation under ambient conditions or the degree of bleaching at the end of the experiment (Fig. 5A,B,D). A marginally significant negative relationship was detected between community diversity and the degree of parasitism at the end of the experiment, where a more diverse community was associated with a greater degree of symbiont parasitism ($R^2 = 0.56$, $P = 0.054$, Fig 5C). We did not detect any relationships between the percent of Clade D in the symbiont community and symbiont density on day 2, mean carbon translocation under ambient conditions, or the degree of parasitism or bleaching at the end of the experiment (Fig. 5E-H), but this was likely due to the fact that the abundance of D was very low in all species except *G. acrhelia*. *G. acrhelia,* however, did exhibit the highest carbon translocation rates under ambient conditions and the greatest transition towards parasitism on day 17 (Fig. 5F,G).

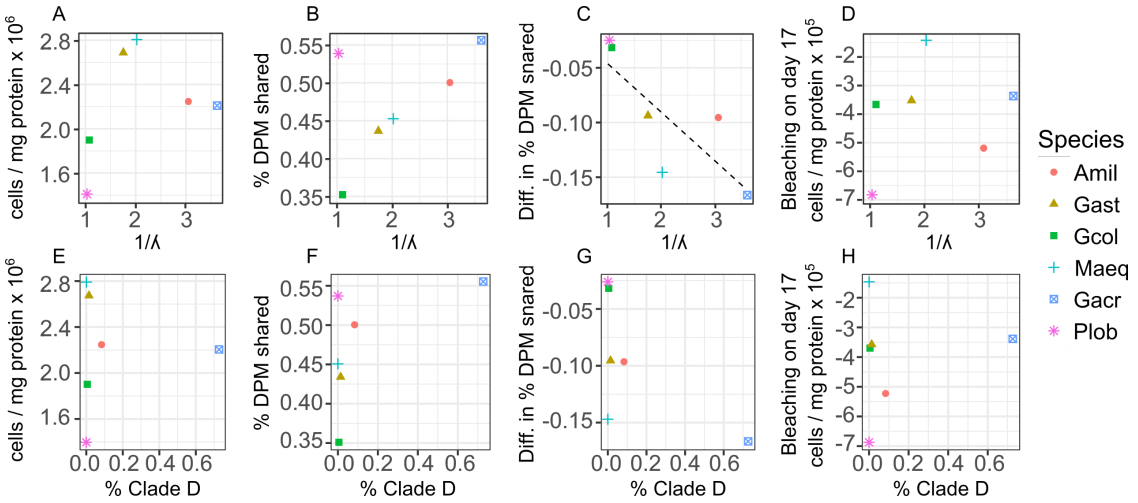

Figure 5. Relationships between changes in symbiont cell density or the proportion of photosynthetically fixed carbon translocated to hosts as a function of symbiont community diversity, expressed as the inverse Simpson index (A-D) or the normalized proportion of Clade D *Symbiodinium* (E-H) across species. For the dependent variables: (A,E) mean symbiont cell density in heat-treated corals (31°C) on day 2; (B,F) mean proportion of photosynthetically fixed carbon translocated to hosts under ambient conditions (27°C); (C,G) The degree of symbiont parasitism, calculated as the difference in the proportion of photosynthetically fixed carbon translocated to hosts between control and heat-treated corals on day 17.

428 DISCUSSION

429 Understanding variation in the degree of cooperation between corals and their
430 *Symbiodinium* will be critical for assessing survival potential among species and populations
431 in the face of increasing environmental change (Lesser et al. 2013). As in other mutualisms
432 (Ebert 2013; Frank 1994; Herre et al. 1999), vertical transmission has been proposed as an
433 evolutionary mechanism for enhancing holobiont fitness in the Cnidarian-algal symbiosis
434 (Putnam et al. 2012). However, we did not observe universally consistent differences in
435 cooperation between vertical and horizontally transmitting species. The vertically
436 transmitting *P. lobata* and *G. acrhelia* exhibited the highest levels of carbon translocation in
437 ambient conditions, which we interpret as symbiont-host cooperation, significantly more so
438 than their respective horizontally-transmitting counterparts, *G. columna* and *G. astreata*; but
439 cooperation was not different between *M. aequituberculata* and *A. millepora*, and tended to
440 be higher in the latter horizontally transmitting species. However, species-specific
441 photosynthesis-irradiance curves were not measured and the potential for interactions
442 between photophysiology and baseline rates of carbon translocation must also be explored.
443 We also expected that the degree of breakdown in the host-symbiont relationship under heat
444 stress, which we interpret as a transition towards parasitism *sensu* (Baker et al. 2018), would
445 be comparatively intensified in horizontally transmitting species, but again, this was not the
446 case. *P. lobata* did exhibit the least change in carbon translocation in spite of showing the
447 same signs of bleaching as other species, but there was no difference in comparison to *G.*
448 *columna* which also largely maintained its baseline translocation under elevated temperature.
449 In addition, the greatest relative declines in the proportion of carbon translocated from
450 symbionts to hosts actually occurred in the other two vertically transmitting species, *G.*
451 *acrhelia* and *M. aequituberculata*.

452 Although we did not find significant support for the role of vertical transmission we
453 still observed significant differences in cooperation among our six focal species, both
454 baseline differences under ambient conditions and in the degree of transition towards
455 parasitism under elevated temperature stress. We therefore conducted a series of *post hoc*
456 analyses to explore other putative drivers of differential cooperation and thermal tolerance:
457 differences in *Symbiodinium* cell density and/or in symbiont community composition.

458 The density of symbiont cells was recently proposed as a major driver underpinning
459 the degree of cooperation between coral hosts and symbionts and the functional response of
460 the coral symbiosis to environmental stressors (Cunning & Baker 2014). Studies in other
461 species have shown that corals with greater initial *Symbiodinium* cell densities, as quantified
462 by the symbiont to host cell ratio, are subsequently associated with greater bleaching severity
463 in response to elevated thermal stress (Cunning & Baker 2013; Silverstein et al. 2014). This
464 association has been hypothesized to result from the proportional increase in oxidative
465 cellular stress: more symbionts yield more reactive oxygen species when the photosynthetic
466 machinery is overloaded (Cunning & Baker 2014), though the recent work of Baker et al.
467 (Baker et al. 2018), adds another potential explanation. They showed that under non-limiting
468 nutrient conditions, *Symbiodinium* cell division in *Orbicella faveolata* actually increased in
469 response to sub-bleaching temperature exposure, but that the metabolic costs were borne by
470 the coral hosts (Baker et al. 2018), supporting the prediction that a transition to parasitism
471 precedes unsustainable proliferation of the symbiont community which ultimately results in
472 bleaching (Wooldridge 2009).

473 In examining relationships between symbiont cell densities, the intensity of the
474 bleaching response at the end of our 17-day temperature exposure and carbon translocation
475 rates, we did observe a negative relationship between initial symbiont cell density on days 2
476 and 4 and subsequent bleaching response on day 17, which did not significantly differ among

477 our six focal species. However, initial symbiont cell densities did not predict the degree of the
478 subsequent transition to parasitism. In fact, the majority of species showed a trend in which
479 greater initial cell densities were associated with a greater maintenance of cooperation under
480 bleaching stress. We also found no relationship between the degree of bleaching and the
481 degree of parasitism on day 17, nor did symbiont cell density explain variation in cooperation
482 among species in ambient conditions. For some species, cooperation tended to decrease with
483 increasing density of symbionts, whereas in others it increased. Taken together, these
484 observations support the association between initial symbiont cell density and subsequent
485 bleaching intensity, but disagree with the proposed role of an alteration of host-symbiont
486 cooperation in mediating the bleaching response.

487 The discrepancy in results among studies may be due to the importance of nutrient
488 enrichment for observing a parasitic increase in symbiont communities, or in the difference in
489 study duration and sampling design. Corals were exposed to a constant light environment,
490 which likely did not provide a saturating irradiance across species. Consequently, alteration
491 of carbon translocation as a function of species-specific photophysiology may explain
492 baseline differences in ambient conditions, and future work should aim to test this hypothesis.
493 In addition, while corals received supplemental feeding throughout the duration of this
494 experiment, which likely introduced organic nitrogen, we did not explicitly manipulate
495 inorganic nitrogen levels. It is also possible that variation among hosts in their ability to limit
496 their symbionts' nitrogen supply may have influenced the observed variation in the degree of
497 parasitism (Cunning et al. 2017; Wooldridge 2009), though additional studies are needed to
498 test this. In addition, Baker et al. (Baker et al. 2018) exposed corals to a +5°C temperature
499 ramp over 8 days, sampling once 24 hours after the final temperature was reached, whereas
500 the present study increased temperatures by +4°C over 5 days and maintained that difference
501 for an additional 12 days, sampling at three time points, comparatively earlier and later. We

502 did not observe an initial increase in symbiont cell density or decrease in carbon translocation
503 on days 2 and 4 under elevated temperature, the experimental time-frame most analogous to
504 that of Baker et al. (Baker et al. 2018). It is possible that these dynamics occurred during a
505 time frame in which we did not sample; however, our final results argue against this
506 explanation. On day 17, we observed symptoms of bleaching that did not differ across
507 species: symbiont cell densities and rates of net photosynthesis were uniformly decreased.
508 However, the transition to parasitism was not uniform, as some species exhibited significant
509 differences in carbon translocation in response to heat stress whereas others did not. We
510 therefore conclude that while symbiont density alone may be a reasonable predictor of the
511 potential for observing a bleaching response under elevated temperature, it does not predict
512 cooperative dynamics that likely also influence holobiont fitness.

513 We therefore also explored the role of symbiont community diversity on bleaching
514 stress and cooperation. Predictions regarding the cooperative and fitness benefits of evolving
515 vertical transmission are based on the assumption that the host-symbiont relationship
516 becomes exclusive: symbiont population sizes are substantially reduced, resulting in genetic
517 uniformity, more rapid co-evolution of partner traits and reduction in intra-symbiont
518 community competition (Herre et al. 1999; Maynard Smith & Szathmary 1995). In this case,
519 it may not be vertical transmission *per se* that influences host-symbiont cooperation, but the
520 relative diversity of the symbiont community. A prior meta-analysis found that symbiont
521 specificity was correlated with transmission mode, with horizontally transmitting species
522 being more likely to interact with generalist symbionts (Fabina et al. 2012). However, the
523 relationship between transmission mode and overall community diversity was not explored.
524 Other more recent studies have also shown the potential for ontogenetic shifts in
525 *Symbiodinium* community composition of putative vertical transmitters, potentially indicating
526 the capacity for mixed-mode or cryptic horizontal transmission (Byler et al. 2013; Reich et al.

527 2017). Our results show that symbiont diversity does not partition by transmission mode.
528 While communities in the vertically transmitting *M. aequituberculata* and *P. lobata* were
529 largely uniform, consisting predominantly of C35 and C15-type sequence variants,
530 respectively, *Symbiodinium* community diversity was more than twice as high in *G. acrhelia*
531 in comparison to *G. astreata* (1/D = 3.6 vs. 1.7). In addition, community composition in the
532 horizontally transmitting *G. columna* was also highly uniform, second only to that of *P.*
533 *lobata* (1/D = 1.08 and 1.00, respectively).

534 In exploring the relationship between symbiont diversity at the ITS2 locus and metrics
535 of host-symbiont cooperation and bleaching independent of transmission mode, we did not
536 find any formally significant correlations, likely due to the fact that our symbiont community
537 analysis was limited to the level of differences among the six species, greatly reducing our
538 statistical power. However, there was a weak negative relationship between community
539 diversity and the degree of parasitism under thermal stress. Species with the most genetically
540 uniform symbiont communities, *P. lobata* and *G. columna*, maintained the highest levels of
541 cooperation in spite of showing signs of bleaching. Yet there was no relationship between
542 community diversity and baseline differences in cooperation among species under ambient
543 conditions, as high rates of translocation were observed in species with both the lowest (*P.*
544 *lobata*) and highest community diversity (*A. millepora, G. acrhelia*), though again, species-
545 specific interactions between photophysiology and carbon translocation remain to be
546 explored.

547 The presence of particular symbiont types has also been shown to influence holobiont
548 fitness and carbon translocation. For example, conspecific corals hosting clade D
549 *Symbiodinium* exhibit greater thermal tolerance than those hosting C1 or C2-types
550 (Berkelmans & van Oppen 2006; Jones et al. 2008), however they generally grow more
551 slowly under non-stressful conditions (Jones & Berkelmans 2010; Little et al. 2004) and

552 receive less photosynthetically fixed carbon from their symbionts (Cantin et al. 2009). We
553 found no significant relationships between the proportional abundance of Clade D-type
554 symbionts and metrics of host-symbiont cooperation or bleaching. Most species had no, or a
555 low proportion of Clade D, but the species with the greatest proportion of Clade D symbionts
556 (*G. acrhelia*) exhibited both the highest carbon translocation under ambient conditions and
557 the greatest transition to parasitism under elevated temperature stress. Similar to our
558 observations regarding symbiont cell density, these results support prior observations that
559 *Symbiodinium* community composition alone is not sufficient to explain variation in
560 holobiont performance (Abrego et al. 2008; Baird et al. 2009a; Kenkel et al. 2013). However,
561 we reiterate that our analyses are limited in comparing only averages among species. There
562 was some variation observed in dominant symbiont types among individual coral colonies
563 within species (Fig. S6) and a priority for future study should be to investigate whether these
564 conclusions hold when considering intraspecific variation in symbiont community
565 composition in addition to these broader interspecific differences.

566 Quantifying cooperation between symbiotic partners in terms of biologically realistic
567 costs and benefits remains an outstanding question for many symbioses (Herre et al. 1999).
568 The transfer of photosynthetically fixed carbon has long been known as a major cooperative
569 benefit to the coral host as up to 95% of a coral's energy requirements can be met through
570 this mechanism (Muscatine 1990); however, reciprocal products shared by hosts with their
571 symbionts remain largely unknown (Yellowlees et al. 2008). Similarly, heterotrophic feeding
572 can offset the need for symbiont-derived carbon in some species and in these cases other
573 symbiont-derived metabolites may be more critical for host fitness (Grottoli et al. 2006).
574 Substantial variation in both intra- and inter-specific bleaching thresholds (Marshall & Baird
575 2000), suggests that levels of cooperation between host and symbiont may also vary.
576 Significant work has gone into investigating coral bleaching over the past three decades, yet

fundamental questions remain unresolved (Edmunds & Gates 2003). Ultimately, a greater understanding of both fine-scale interactions between coral hosts and symbionts and the evolutionary and ecological mechanisms that maintain and strengthen cooperation will be essential for managing these ecosystems (Davy et al. 2012; Lesser et al. 2013).

CONCLUSIONS

This study investigated whether corals employing vertical symbiont transmission also exhibit enhanced cooperation and holobiont fitness. Contrary to theoretical predictions, we did not find significant support for the role of vertical transmission in spite of significant differences in cooperation among our six focal species. In a *post hoc* analysis of other drivers, we found that a greater initial symbiont cell density was associated with a greater bleaching intensity, but this association did not appear to result from an alteration of host-symbiont cooperation. Rather, the reduction in cooperation across species at the onset of bleaching was marginally associated with symbiont community diversity. The theoretical benefits of evolving vertical transmission are based on the underlying assumption that the host-symbiont relationship becomes genetically uniform, thereby reducing competition among symbionts. Taken together, our results suggest that it may not be vertical transmission *per se* that influences host-symbiont cooperation, but genetic uniformity of the symbiont community, though future work is needed to directly test this hypothesis.

ACKNOWLEDGEMENTS

The authors gratefully acknowledge the efforts of A Bouriat in maintaining aquaria and processing coral samples. M Salmon, G Milton, A Severati, C Humphrey implemented the experimental aquaria design. Coral collection was accomplished with the help of S Noonan, V Mocellin, A Severati and M Nayfa. P Muir provided advice on coral taxonomic identification. Comments from J Caley, B Schaffelke and multiple anonymous reviewers greatly improved this manuscript.

620 REFERENCES

621 Abrego D, Ulstrup KE, Willis BL, and van Oppen MJH. 2008. Species-specific interactions between
622 algal endosymbionts and coral hosts define their bleaching response to heat and light stress.
623 *Proceedings of the Royal Society B-Biological Sciences* 275:2273-2282.
624 10.1098/rspb.2008.0180
625 Anders S, and Huber W. 2010. Differential expression analysis for sequence count data. *Genome*
626 *Biology* 11:R106.
627 Anderson RM, and May RM. 1982. Coevolution of hosts and parasites. *Parasitology* 85:411-426.
628 Anthony KRN, Kline DI, Diaz-Pulido G, Dove S, and Hoegh-Guldberg O. 2008. Ocean acidification
629 causes bleaching and productivity loss in coral reef builders. *Proceedings of the National*
630 *Academy of Sciences of the United States of America* 105:17442-17446.
631 10.1073/pnas.0804478105
632 Baird AH, Bhagooli R, Ralph PJ, and Takahashi S. 2009a. Coral bleaching: the role of the host. *Trends*
633 *in Ecology & Evolution* 24:16-20. 10.1016/j.tree.2008.09.005
634 Baird AH, Guest JR, and Willis BL. 2009b. Systematic and Biogeographical Patterns in the
635 Reproductive Biology of Scleractinian Corals. *Annual Review of Ecology Evolution and*
636 *Systematics* 40:551-571. 10.1146/annurev.ecolsys.110308.120220
637 Baker AC, and Rowan R. 1997. Diversity of symbiotic dinoflagellates (zooxanthellae) in scleractinian
638 corals fo the Caribbean and Eastern Pacific. Proceedings of the 8th International Coral Reef
639 Symposium. p 1301-1306.
640 Baker DM, Freeman CJ, Wong JCY, Fogel ML, and Knowlton N. 2018. Climate change promotes
641 parisitism in a coral symbiosis. *The ISME Journal*. https://doi.org/10.1038/s41396-018-
642 0046-8
643 Benjamini Y, and Hochberg Y. 1995. Controlling the false discovery rate - a practical and powerful
644 approach to multiple testing. *Journal of the Royal Statistical Society Series B-Methodological*
645 57:289-300.
646 Berkelmans R, and van Oppen MJH. 2006. The role of zooxanthellae in the thermal tolerance of
647 corals: a 'nugget of hope' for coral reefs in an era of climate change. *Proceedings of the*
648 *Royal Society B-Biological Sciences* 273:2305-2312. 10.1098/rspb.2006.3567
649 Bright M, and Bulgheresi S. 2010. A complex journey: transmission of microbial symbionts. *Nature*
650 *Reviews Microbiology* 8:218-230.
651 Brown BE. 1997. Coral bleaching: causes and consequences. *Coral Reefs* 16:S129-S138.
652 Bull JJ. 1994. Perspective: virulence. *Evolution* 48:1423-1437.
653 Bull JJ, Molineux IJ, and Rice WR. 1991. Selection of benevolence in a host-parasite system. *Evolution*
654 45:857-882.
655 Byler KA, Carmi-Veal M, Fine M, and Goulet TL. 2013. Multiple symbiont acquisition strategies as an
656 adaptive mechanism in the coral Stylophora pistillata. *PLoS ONE* 8:e59596.
657 Callahan BJ, McMurdie, Paul J, Rosen, Michael J, Han, Andrew W, Johnson, Amy Jo A, Holmes, Susan
658 P. 2016. DADA2: High-resolution sample inference from Illumina amplicon data. *Nature*
659 *Methods* 13:581-583.
660 Cantin NE, van Oppen MJH, Willis BL, Mieog JC, and Negri AP. 2009. Juvenile corals can acquire more
661 carbon from high-performance algal symbionts. *Coral Reefs* 28:405-414. 10.1007/s00338-
662 009-0478-8
663 Cunning R, and Baker AC. 2013. Excess of algal symbionts increase the susceptibility of reef corals to
664 bleaching. *Nature Climate Change* 3:259-262.
665 Cunning R, and Baker AC. 2014. Not just who, but how many: the importance of partner abundance
666 in reef coral symbioses. *Frontiers in Microbiology* 5. 10.3389/fmicb.2014.00400
667 Cunning R, Muller EB, Gates RD, and Nisbet RM. 2017. A dynamic bioenergetic model for coral-
668 Symbiodinium symbioses and coral bleaching as an alternate stable state. *Journal of*
669 *Theoretical Biology* 431:49-62. 10.1016/j.jtbi.2017.08.003

670 Daly M, Brugler MR, Cartwright P, Collines AG, Dawson MN, Fautin DG, France SC, McFadden CS,
671 Opresko DM, Rodriguez E, Romano SL, and Stake JL. 2007. The phylum Cnidaria: A review of
672 phylogenetic patterns and diversity 300 years after Linnaeus. In: Zhang ZQ, and Shear WA,
673 eds. *Linnaeus Tercentenary: Progress in Invertebrate Taxonomy*: Zootaxa, 127-182.
674 Davy SK, Allemand D, and Weis VM. 2012. Cell biology of Cnidarian-dinoflagellate symbiosis.
675 *Microbiology and Molecular Biology Reviews* 76:229-261.
676 Doebeli M, and Knowlton N. 1998. The evolution of interspecific mutualisms. *Proceedings of the*
677 *National Academy of Sciences of the United States of America* 95:8676-8680.
678 Dusi E, Gougat-Barbera C, Berendonk TU, and Kaltz O. 2015. Long-term selection experiment
679 produces breakdown of horizontal transmissibility in parasite with mixd transmission mode.
680 *Evolution* 69:1069-1076.
681 Ebert D. 2013. The epidemiology and evolution of symbionts with mixed-mode transmission. *Annual*
682 *Review of Ecology, Evolution, and Systematics* 44:7.1-7.21.
683 Ebert D, and Bull JJ. 2003. Challenging the trade-off model for the evolution of virulence: is virulence
684 management feasible? *Trends in Microbiology* 11:15-20.
685 Edmunds PJ, and Gates RD. 2003. Has coral bleaching delayed our understanding of fundamental
686 aspects of coral-dinoflagellate symbioses? *BioScience* 53:976-980.
687 Fabina NS, Putnam HM, Franklin EC, Stat M, and Gates RD. 2012. Transmission mode predicts
688 specificity and interaction patterns in coral-Symbiodinium networks. *PLoS ONE* 7:e44970.
689 doi10.1371/journal.pone.0044970
690 Frank SA. 1994. Genetics of mutualism: the evolution of altruism between species. *Journal of*
691 *Theoretical Biology* 170:393-400.
692 Franklin EC, Stat M, Pochon X, Putnam HM, and Gates RD. 2012. GeoSymbio: a hybrid, cloud-based
693 web application of global geospatial bioinformatics and ecoinformatics for Symbiodinium-
694 host symbioses. *Molecular Ecology Resources* 12:369-373.
695 Friesen ML, and Jones EI. 2013. Modelling the evolution of mutualistic symbioses. In: van Helden J,
696 Toussaint A, and Thieffry D, eds. *Bacterial Molecular Networks: Methods and Protocols*:
697 Springer Science+Business Media, 481-499.
698 Frøslev TG, Kjøller R, Bruun HH, Ejrnæs R, Brunbjerg AK, Pietroni C, and Hansen AJ. 2017. Algorithm
699 for post-clustering curation of DNA amplicon data yields reliable biodiversity estimates.
700 *Nature Communications* 8:1188. 10.1038/s41467-017-01312-x
701 Green EA, Davies SW, Matz MV, and Medina M. 2014. Quantifying cryptic Symbiodinium diversity
702 with Orbicella faveolata and Orbicella franksi at the Flower Garden Banks, Gulf of Mexico.
703 *PeerJ* 2:e386. 10.7717/peerj.386
704 Grottoli AG, Rodrigues LJ, and Palardy JE. 2006. Heterotrophic plasticity and resilience in bleached
705 corals. *Nature* 440:1186-1189. 10.1038/nature04565
706 Harrison PL, and Wallace CC. 1990. Reproduction, dispersal and recruitment of scleractinian corals.
707 In: Dubinsky Z, ed. *Ecosystems of the World: Coral Reefs*. New York: Elsevier, 133-207.
708 Hartmann AC, Baird AH, Knowlton N, and Huang D. 2017. The paradox of environmental symbiont
709 acquisition in obligate mutualisms. *Current Biology* 27:3711-3716.
710 Hatcher BG. 1988. Coral reef primary productivity: A beggar's banquet. *Trends in Ecology and*
711 *Evolution* 3:106-111.
712 Herre EA. 1993. Population structure and the evolution of virulence in nematode parasites of fig
713 wasps. *Science* 259:1442-1445.
714 Herre EA, Knowlton N, Mueller UG, and Rehner SA. 1999. The evolution of mutualisms: exploring the
715 paths between conflict and cooperation. *Trends in Ecology & Evolution* 14.
716 Hoegh-Guldberg O, Mumby PJ, Hooten AJ, Steneck RS, Greenfield P, Gomez E, Harvell CD, Sale PF,
717 Edwards AJ, Caldeira K, Knowlton N, Eakin CM, Iglesias-Prieto R, Muthiga N, Bradbury RH,
718 Dubi A, and Hatziolos ME. 2007. Coral reefs under rapid climate change and ocean
719 acidification. *Science* 318:1737-1742. 10.1126/science.1152509

720 Hughes TP, Baird AH, Bellwood DR, Card M, Connolly SR, Folke C, Grosberg R, Hoegh-Guldberg O,
721 Jackson JBC, Kleypas J, Lough JM, Marshall P, Nystrom M, Palumbi SR, Pandolfi JM, Rosen B,
722 and Roughgarden J. 2003. Climate change, human impacts, and the resilience of coral reefs.
723 *Science* 301:929-933.
724 Johnson PCD. 2014. Extension of Nakagawa & Schielzeth's R2GLMM to random slopes models.
725 *Methods in Ecology and Evolution* 5:944-946.
726 Jones A, and Berkelmans R. 2010. Potential Costs of Acclimatization to a Warmer Climate: Growth of
727 a Reef Coral with Heat Tolerant vs. Sensitive Symbiont Types. *PLoS ONE* 5.
728 10.1371/journal.pone.0010437
729 Jones A, Berkelmans R, van Oppen MJH, Mieog JC, and Sinclair W. 2008. A community change in the
730 algal endosymbionts of a scleractinian coral following a natural bleaching event: field
731 evidence of acclimatization. *Proceedings of the Royal Society B-Biological Sciences* 275:1359-
732 1365.
733 Kenkel C, Goodbody-Gringley G, Caillaud D, Davies SW, Bartels E, and Matz M. 2013. Evidence for a
734 host role in thermotolerance divergence between populations of the mustard hill coral
735 (Porites astreoides) from different reef environments. *Molecular Ecology* 22:4335-4348.
736 Kerr AM, Baird AH, and Hughes TP. 2011. Correlated evolution of sex and reproductive mode in
737 corals (Anthozoa: Scleractinia). *Proceedings of the Royal Society B-Biological Sciences*
738 278:75-81.
739 Kiers TE, and West SA. 2015. Evolving new organisms via symbiosis. *Science* 348:392-394.
740 Knowlton N, Brainard RE, Fisher R, Moews M, Plaisance L, and Caley MJ. 2010. Coral Reef
741 Biodiversity. In: McIntyre A, ed. *Life in the World's Oceans: Diversity, Distribution, and*
742 *Abundance*. Oxford: Blackwell Publishing Ltd., 65-78.
743 LaJeunesse TC. 2002. Diversity and community structure of symbiotic dinoflagellates from Caribbean
744 coral reefs. *Marine Biology* 141:387-400.
745 Lesser MP, Stat M, and Gates RD. 2013. The endosymbiotic dinoflagellates (Symbiodinium sp.) of
746 corals are parasites and mutualists. *Coral Reefs* 32:603-611.
747 Little AF, van Oppen MJH, and Willis BL. 2004. Flexibility in algal endosymbioses shapes growth in
748 reef corals. *Science* 304:1492-1494.
749 Magurran AE. 2004. *Measuring biological diversity*. Oxford, UK: Blackwell Science Ltd.
750 Marshall PA, and Baird AH. 2000. Bleaching of corals on the Great Barrier Reef: differential
751 susceptibilities among taxa. *Coral Reefs* 19:155-163.
752 Maynard Smith J, and Szathmary E. 1995. *The Major Transitions in Evolution*. Oxford: Freeman.
753 Moran NA. 2006. Symbiosis. *Current Biology* 16:R866-R871.
754 Muscatine L. 1990. The role of symbiotic algae in carbon and energy flux in reef corals. In: Dubinsky,
755 ed. *Ecosystems of the world 25: Coral reefs*. New York: Elsiever, 75-87.
756 Nowak MA, Bonhoeffer S, and May RM. 1994. Spatial games and the maintenance of cooperation.
757 *Proceedings of the National Academy of Sciences of the United States of America* 91:4877-
758 4881.
759 Palstra F. 2000. Host-endosymbiont specificity in Acropora corals of the Indo-Pacific? James Cook
760 University.
761 Pinheiro J, Bates D, DebRoy S, Sarkar D, and Team RDC. 2013. nlme: Linear and nonlinear mixed
762 effects models. R package version 3.1-113 ed.
763 Pochon X, Pawlowski J, Zaninetti L, and Rowan R. 2001. High genetic diversity and relative specificity
764 among Symbiodinium-like endosymbiotic dinoflagellates in soritid foraminiferans. *Marine*
765 *Biology* 139:1069-1078.
766 Putnam HM, Stat M, Pochon X, and Gates RD. 2012. Endosymbiotic flexibility associates with
767 environmental sensitivity in scleractinian corals. *Proceedings of the Royal Society B:*
768 *Biological Sciences* 279:4352-4361.
769 Quigley KM, Davies SW, Kenkel CD, Willis BL, Matz MV, and Bay LK. 2014. Deep-Sequencing Method
770 for Quantifying Background Abundances of Symbiodinium Types: Exploring the Rare

771 Symbiodinium Biosphere in Reef-Building Corals. *PLoS ONE* 9:e94297.
772 doi:10.1371/journal.pone.0094297
773 Ralph PJ, Larkum AWD, and Kuhl M. 2005. Temporal patterns in effective quantum yield of individual
774 zooxanthellae expelled during bleaching. *Journal of Experimental Marine Biology and*
775 *Ecology* 316:17-28.
776 Reich HG, Robertson DL, and Goodbody-Gringley G. 2017. Do the shuffle: Changes in Symbiodinium
777 consortia throughout juvenile coral development. *PLoS ONE* 12:e0171768.
778 10.1371/journal.pone.0171768
779 Roth MS. 2014. The engine of the reef: photobiology of the coral-algal symbiosis. *Frontiers in*
780 *Microbiology* 5:422. 10.3389/fmicb.2014.00422
781 Sachs JL, Essenberg CJ, and Turcotte MM. 2011. New paradigms for the evolution of beneficial
782 infections. *Trends in Ecology & Evolution* 26:202-209.
783 Sachs JL, Mueller UG, Wilcox TP, and Bull JJ. 2004. The evolution of cooperation. *Quarterly Review of*
784 *Biology* 79:135-160.
785 Sachs JL, and Wilcox TP. 2006. A shift to parasitism in the jellyfish symbiont Symbiodinium
786 microadriaticum. *Proceedings of the Royal Society B-Biological Sciences* 273:425-429.
787 Silverstein RN, Cunning R, and Baker AC. 2014. Change in algal symbiont communities after
788 bleaching, not prior heat exposure, increases heat tolerance of reef corals. *Global Change*
789 *Biology* 21:236-249.
790 Stanley GD, and Swart PK. 1995. Evolution of the coral-zooxanthellae symbiosis during the Triassic: a
791 geochemical approach. *Paleobiology* 21:179-199.
792 Stewart AD, Logsdon JM, and Kelley SE. 2005. An empirical study of the evolution of virulece under
793 both horizontal and vertical transmission. *Evolution* 59:730-739.
794 Strahl J, Stolz I, Uthicke S, Vogen N, Noonan SHC, and Fabricius KE. 2015. Physiological and ecological
795 performance differs in four coral taxa at a volcanic carbon dioxide seep. *Comparative*
796 *Biochemistry and Physiology Part A: Molecular & Integrative Physiology* 184:179-186.
797 Team RC. 2017. R: A language and environment for statistical computing. Vienna: R Foundation for
798 Statistical Computing.
799 Tonk L, Bongaerts P, Sampayo EM, and Hoegh-Guldberg O. 2013. SymbioGBR: a web-based database
800 of Symbiodinium associated with cnidarian hosts on the Great Barrier Reef. *BMC Ecology* 13.
801 Veal CJ, Carmi M, Fine M, and Hoegh-Guldberg O. 2010. Increasing the accuracy of surface area
802 estimation using single wax dipping of coral fragments. *Coral Reefs* 29:893-897.
803 Wilson K, Li Y, Whan V, Lehnert S, Byrne K, Moore S, Pongsomboon S, Tassanakajon A, Rosenberg G,
804 Ballment E, Fayazi Z, Swan J, Kenway M, and Benzie J. 2002. Genetic mapping of the black
805 tiger shrimp Penaeus monodon with amplified fragment length polymorphism. *Aquaculture*
806 204:297-309.
807 Wooldridge SA. 2009. Water quality and coral bleaching thresholds: formalising the linkage for the
808 inshore reefs of the Great Barrier Reef, Australia. *Marine Pollution Bulletin* 58:745-751.
809 Yellowlees D, Rees T, and Leggat W. 2008. Metabolic interactions between algal symbionts and
810 invertebrate hosts. *Plant, Cell & Environment* 31:679-694.

811

812

813

814

815

816

Supplementary Material: Exploring mechanisms that affect coral cooperation: symbiont transmission mode, cell density and community composition

Carly D. Kenkel and Line K. Bay

837 Table S1. Raw read counts and reads lost during filtering and clustering with DADA2.

Sample	Raw	Input_DADA2	filtered	denoised	merged	tabled	nonchim
AmilAll	35820	35061	31194	31194	28315	28315	24013
Gach1	74818	74054	67294	67294	66374	66301	62896
Gach10	72354	71449	60322	60322	59915	59451	50573
Gach2	74662	74012	63885	63885	62752	62250	50278
Gach3	35176	34552	25626	25626	25323	25140	22602
Gach4	93883	93234	80667	80667	79625	79064	63253
Gach5	30755	30541	26595	26595	26375	26167	22976
Gach6	40510	39898	34705	34705	34374	34019	31309
Gach7	4472	4332	2643	2643	2611	2598	2528
Gach8	33640	33267	29026	29026	28780	28443	26381
Gach9	40512	40026	34308	34308	34026	33542	31669
GachAll	25286	24821	21705	21705	21399	21246	17958
Gast1	1061	942	582	582	581	581	571
Gast10	33882	33390	30573	30573	30231	30212	29162
Gast2	21197	20863	18934	18934	18696	18696	17876
Gast3	20029	19875	18266	18266	18003	18003	17431
Gast4	16471	16248	13906	13906	13741	13558	12598
Gast5	11943	11730	10196	10196	10172	10172	9182
Gast6	45291	44813	40014	40014	39595	39574	38225
Gast7	33652	33320	29961	29961	29883	29883	26478
Gast8	23892	23539	21491	21491	21312	21287	20885
Gast9	734	621	374	374	374	374	337
GastAll	31819	31304	27836	27836	27425	27367	23894
GcolAll	10196	9940	7972	7972	7839	7839	7661
Maqe10	77568	69196	44998	44998	44705	44698	42679
Maqe6	57788	46772	31275	31275	31160	31114	30225
Maqe6b	51170	27633	17137	17137	17074	17047	16564

Maqe7	29361	23378	16091	16091	15970	15970	15338
Maqe7b	17131	16676	11653	11653	11567	11567	11491
Maqe8	72073	43668	29519	29519	29346	29346	27746
Maqe8b	12976	12418	8388	8388	8314	8314	8214
Maqe9	20282	19533	13318	13318	13226	13226	13131
Maqe9b	59314	31986	19854	19854	19715	19715	19002
MaqeAll	14445	14232	11940	11940	11754	11754	10322
Plob6	16697	5454	3630	3630	725	584	561
Plob6b	28036	3924	2461	2461	1354	1294	1184
Plob7	1469	454	263	263	44	30	3
Plob7b	17267	1798	1135	1135	197	109	109
Plob8b	36191	19086	12600	12600	11986	11940	11837
PlobAll	31619	30869	27527	27527	26407	26341	21754

Table S2. Best BLASTn matches to the GeoSymbio ITS2 database (Franklin et al. 2012) for curated amplicon sequence variants (ASVs) detected across samples. Value in % column indicates mean percent abundance across all samples in which the sequence variant, or sub-variants (identified through LULU curation), were identified. Match bit-scores are reported and hits separated by '/' in GeoSymbio column indicate equally high scoring blast matches.

ASV	%	Score	GeoSymbio BLAST
Sq1	31.6	523	C1
Sq2	18.8	501	D1
Sq3	10.6	508	C35(type2)/C26.b1
Sq4	7.0	501	D1a
Sq5	11.4	508	C35a(type2)/C26a/C26
Sq6	6.6	512	C35(type2)/C26.b1
Sq7	3.8	501	D6
Sq8	4.9	523	C3/Cspc
Sq10	2.5	512	C35a(type2)/C26a/C26
Sq18	1.6	520	C15
Sq23	0.8	523	C15
Sq40	0.3	523	C15a

Table S3. Wald test statistics for individual factors and interaction terms for the *Symbiodinium* cell density model. Significant terms are shown in bold.

	numDF	denDF	F-value	p-value
(Intercept)	1	270	1.989512e+05	0.0000000
Species	**5**	**52**	**9.116880e+00**	**0.0000028**
Temp	**1**	**270**	**1.260908e+01**	**0.0004528**
Day	**2**	**270**	**6.089511e+00**	**0.0025898**
Species:Temp	5	270	1.104898e+00	0.3580558
Species:Day	10	270	1.452625e+00	0.1573259
Temp:Day	**2**	**270**	**1.388694e+01**	**0.0000018**
Species:Temp:Day	10	270	4.876186e-01	0.8975041

Table S4. Wald test statistics for individual factors and interaction terms for the net photosynthesis model. Significant terms are shown in bold.

	numDF	denDF	F-value	p-value
(Intercept)	1	270	1648.4748360	0.0000000
Species	**5**	**52**	**40.2840568**	**0.0000000**
Temp	1	270	3.4308423	0.0650808
Day	**2**	**270**	**5.7878681**	**0.0034574**
Species:Temp	5	270	1.2021088	0.3084131
Species:Day	10	270	0.8998245	0.5338268
Temp:Day	**2**	**270**	**36.4032169**	**0.0000000**
Species:Temp:Day	10	270	1.0755283	0.3486423

Table S5. Wald test statistics for individual factors and interaction terms for the fraction of DPM shared model. Significant terms are shown in bold.

	numDF	denDF	F-value	p-value
(Intercept)	1	120	5585.5585773	0.0000000
Species	**5**	**22**	**18.7172944**	**0.0000003**
Temp	**1**	**120**	**18.0748728**	**0.0000423**
Day	**2**	120	**24.4071621**	**0.0000000**
Species:Temp	**5**	**120**	**3.4767095**	**0.0057086**
Species:Day	10	120	0.6096878	0.8031208
Temp:Day	**2**	120	**14.5121654**	**0.0000023**
Species:Temp:Day	10	120	0.8893596	0.5453031

Figure S1. Daily measures of effective quantum yield (mean EQY±SEM, note that range of error bars is extremely small, in most cases barely exceeding points) of *Symbiodinium* photosystem II by temperature treatment. Bars show the difference in mean EQY between treatments through time (n=720 per bar).

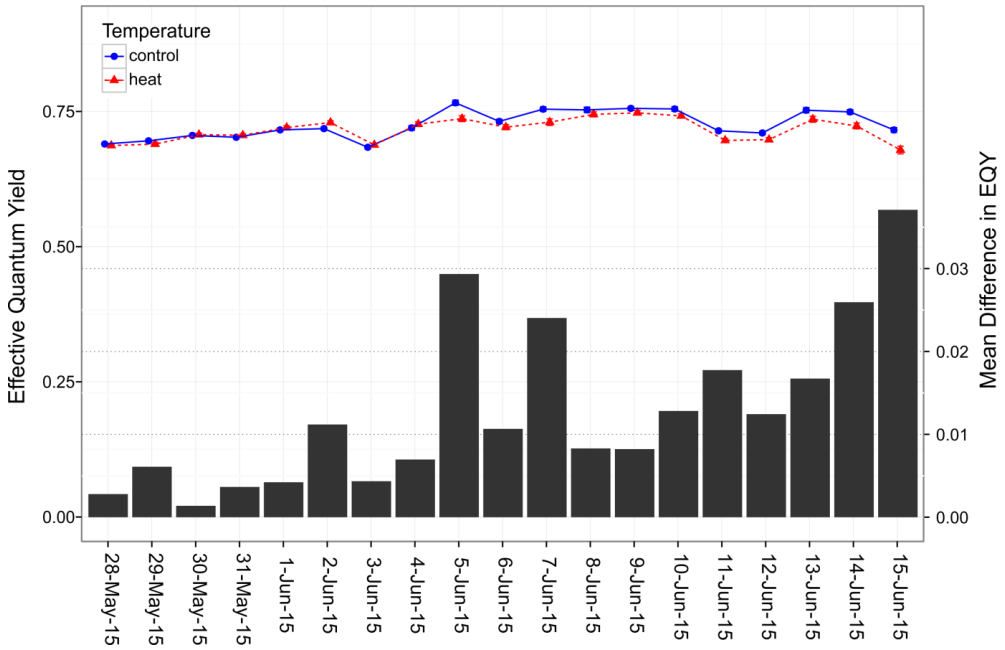

Figure S2. Daily measures of effective quantum yield (EQY±SEM) of *Symbiodinium* photosystem II by temperature treatment and species.

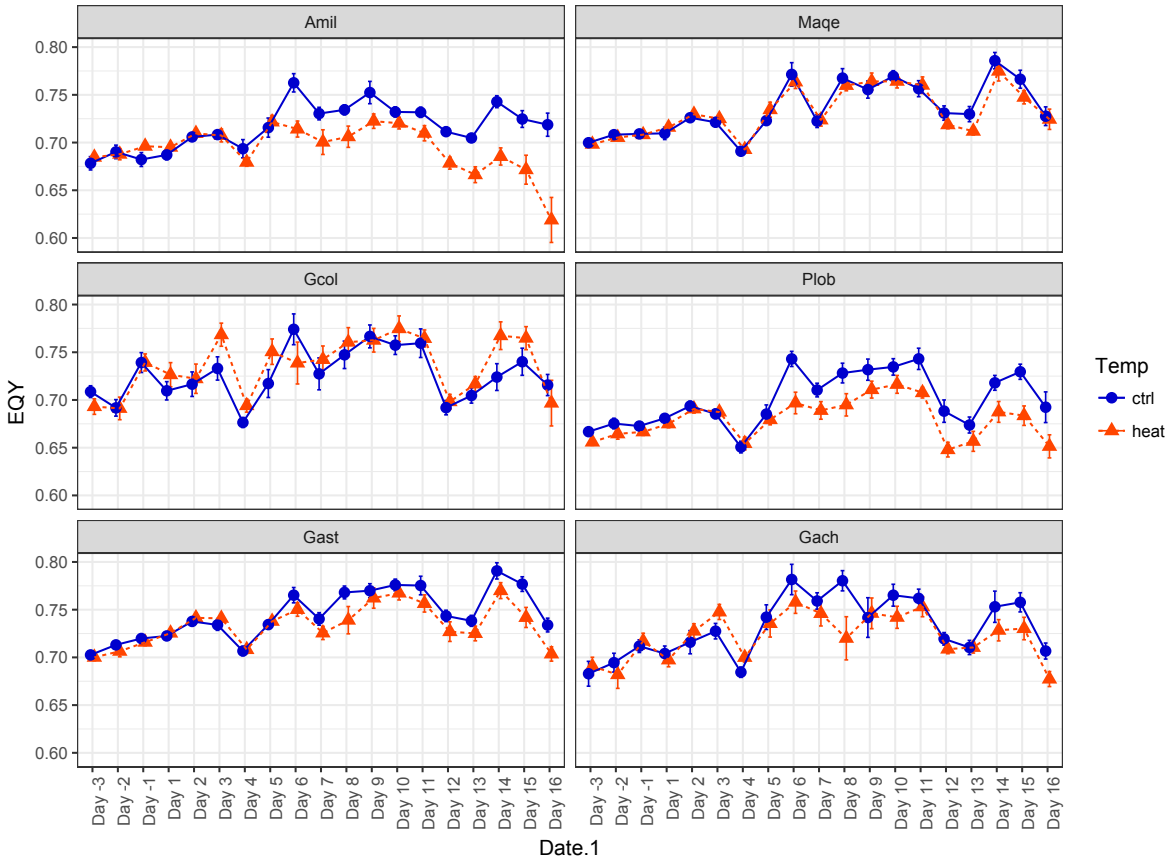

Figure S3. Temperature profile of experimental treatment tanks (±SD) by date. Bars indicate time of sampling.

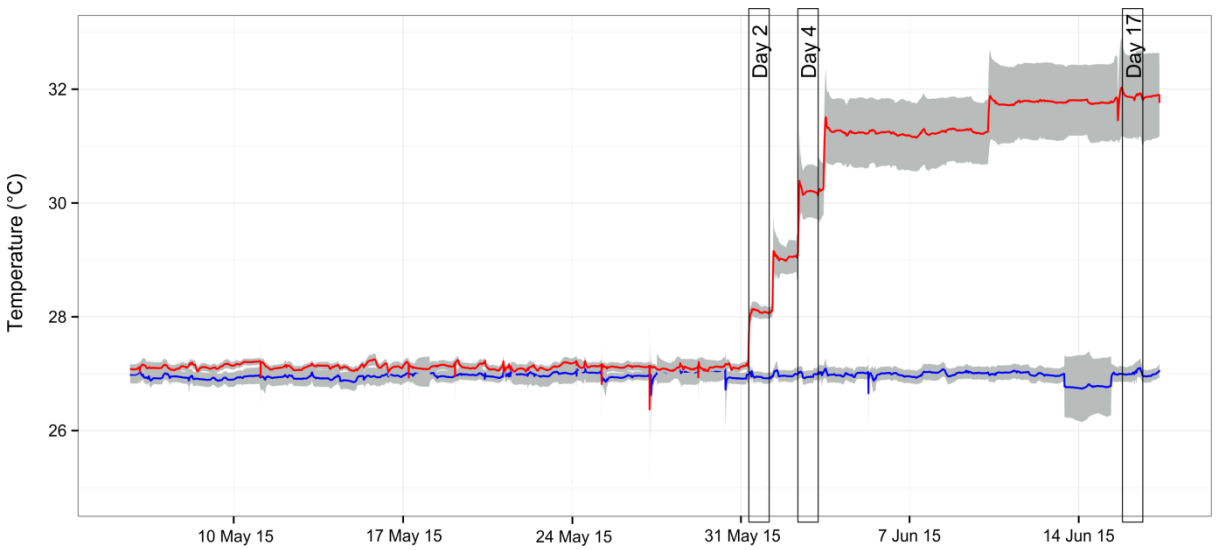

928 Figure S4. *Symbiodinium* cell density, expressed as cells per cm^2 of coral surface area of focal coral
929 species (Amil: *Acropora millepora*, Maeq: *Montipora aequituberculata*, Gcol: *Goniopora columna*,
930 Plob: *Porites lobata*, Gast: *Galaxea astreata*, Gacr: *Galaxea acrhelia*) under control (27°C, blue
931 circles) and elevated (31°C, red triangles) temperature following 2, 4 and 17 days of treatment.

932

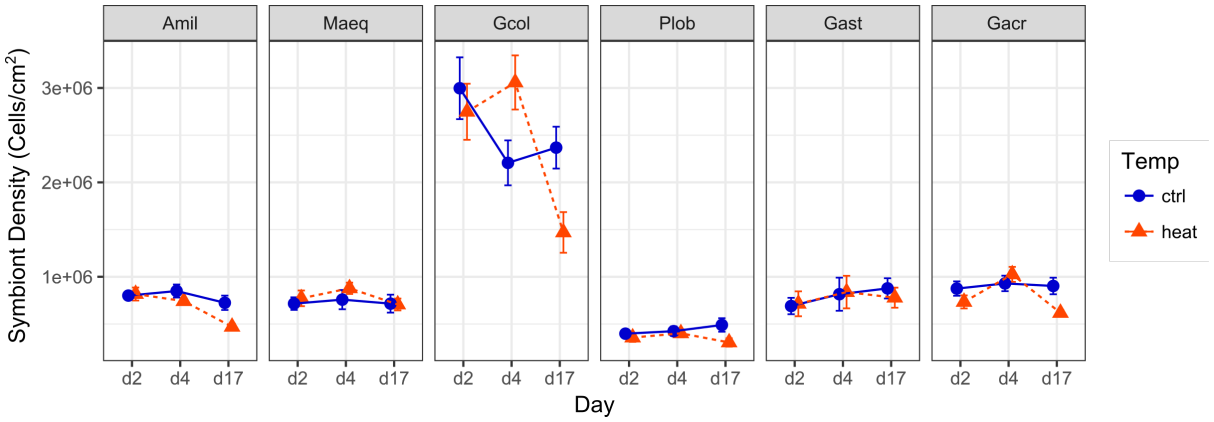

933

934 Figure S5. Taq1 digest of *Symbiodinium* LSU rRNA. Samples are grouped by species pairs. Standard
935 shows expected banding pattern for *Symbiodinium* genotypes in clades C and D.

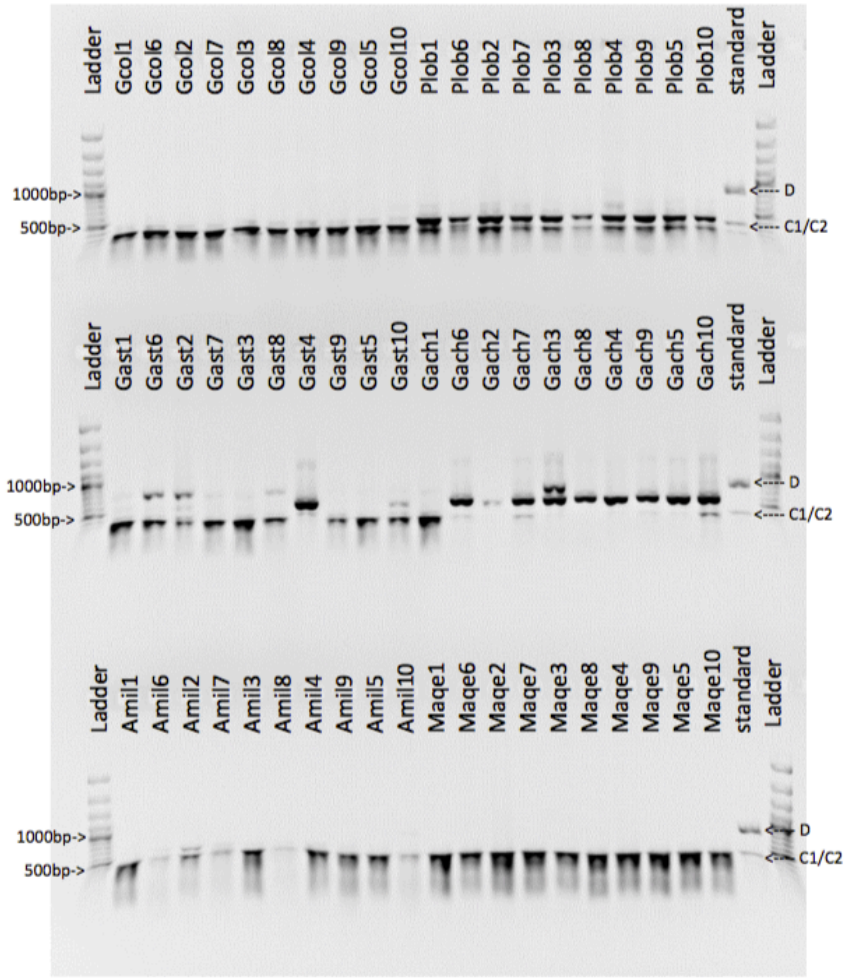

936

Fig S6. Normalized proportional abundance of sequence variants by samples sequenced at UT Austin's GSAF (All and individual Gast/Gacr samples) and OSU's CGRB (individual Maeq and Plob samples). Gacr1 and Gast4 were excluded from subsequent analyses as they appear to be mis-labeled and for analyses comparing differences among species, the 'All' samples for Gacr, Gast, Maeq and Plob were replaced by *in silico* averages calculated using the individual sample replicates shown here.

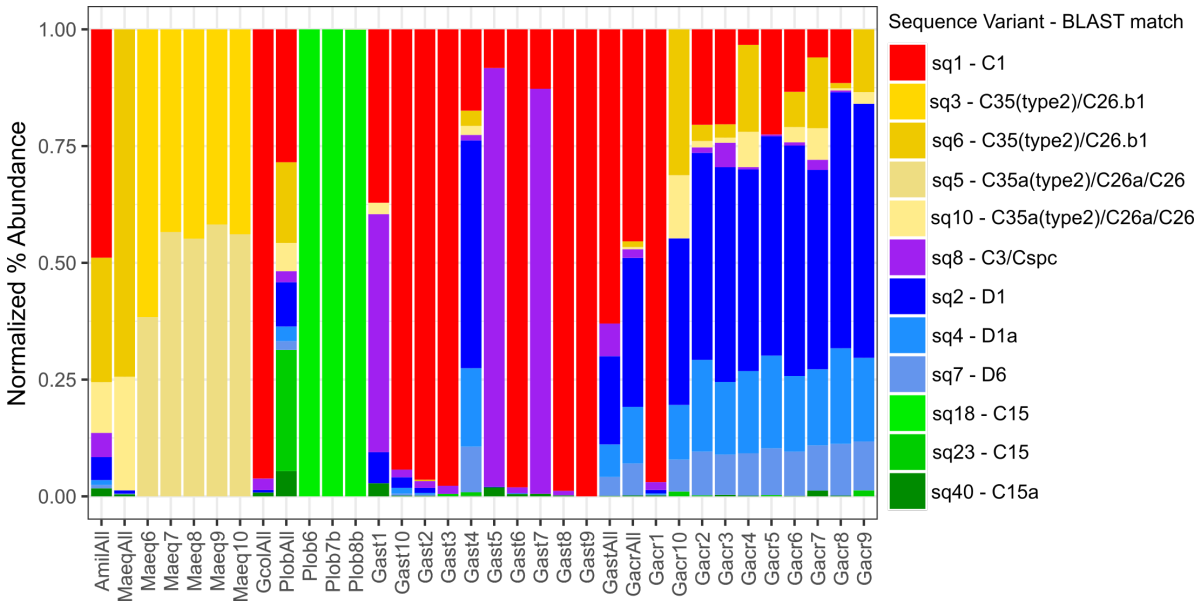

REFERENCES

Franklin, E. C., M. Stat, X. Pochon, H. M. Putnam, and R. D. Gates. 2012. GeoSymbio: a hybrid, cloud-based web application of global geospatial bioinformatics and ecoinformatics for Symbiodinium-host symbioses. Molecular Ecology Resources 12:369-373.

Veal, C. J., M. Carmi, M. Fine, and O. Hoegh-Guldberg. 2010. Increasing the accuracy of surface area estimation using single wax dipping of coral fragments. Coral Reefs 29:893-897.